



OPEN

Dual immobilization of magnetite nanoparticles and biosilica within alginate matrix for the adsorption of Cd(II) from aquatic phase

Mahdi Safari^{1,2}, Reza Rezaee^{1,2}, Reza Darvishi Cheshmeh Soltani³ & Esrafil Asgari⁴✉

The adsorption of cadmium ions by magnetite (Fe₃O₄)@biosilica/alginate (MBA nano-hybrid) was the main aim of the present investigation. Herein, MBA nano-hybrid was synthesized via chemical precipitation technique. As-synthesized MBA nano-hybrid was characterized using FT-IR, FESEM and XRD analyzes. Based on the results, the maximum adsorption capacity of the adsorbent for the removal of Cd(II) was obtained at the initial pH of 7.0. At the initial Cd(II) concentration of 40 mg/L, increasing the reaction time to 180 min led to the Cd adsorption of 35.36 mg/g. Since the removal of Cd(II) after the reaction time of 60 min was insignificant, the reaction time of 60 min was considered as optimum reaction time for performing the experimental runs. According to the results, Langmuir isotherm and pseudo-second order kinetic models were the best fitted models with high correlation coefficients ($R^2 > 0.99$). The results of thermodynamic study indicated exothermic (positive ΔH°) and spontaneous nature (negative ΔG°) of the adsorption of Cd(II) on the surface of MBA nano-hybrid. Negligible reduction in the adsorption capacity of the nano-hybrid was observed (16.57%) after fifth experimental runs, indicating high reusability potential of the as-synthesized nano-hybrid adsorbent.

Pollution of water resources due to the uncontrolled discharge of industrial wastewaters has become a global health and environmental concern¹. Heavy metals are among the most important pollutants in industrial effluents due to their characteristics such as non-degradability, durability, aggregation, and toxicity²⁻⁴. Cadmium, chromium, copper, zinc, and nickel are among the most common heavy metals available in high concentrations in industrial wastewaters^{5,6}.

Cadmium can enter aqueous environment from various sources including non-ferrous metals production, electroplating of metals, battery manufacturing, paint industry, photography, and lead and zinc mines. In addition, volcanic eruptions and forest fires are among the most important natural sources of cadmium entry into the environment^{1,7,8}. Among the heavy metals, much attention is paid to cadmium, due to high toxicity and being categorized as Group B1 (probable human carcinogen compound) by the U.S. Environmental Protection Agency (U.S. EPA)^{9,10}. Cadmium can be bio accumulated like other heavy metals causing cancer even at lower concentrations⁷. Studies showed that exposure to various concentrations of cadmium can lead to acute and chronic complications in the kidney, liver, nervous, and cardiovascular systems¹. The World Health Organization (WHO) has established a maximum concentration level (MCL) of 0.003 mg/L for cadmium in potable water¹¹.

Due to the health problems associated with the presence of cadmium in water, development of effective methods for the removal of cadmium is crucial. Various treatment methods have been utilized to eliminate cadmium ions from water including chemical precipitation, membrane technologies, biological processes, electrochemical techniques, flotation, ion exchange, and adsorption process¹¹. Among the aforementioned methods, the adsorption process is considered among researchers as an economic and appropriate process for the elimination of heavy metal ions from liquid phase due to its simplicity, reliability, and safety^{2,11,12}. Various adsorbents such as activated

¹Environmental Health Research Center, Research Institute for Health Development, Kurdistan University of Medical Sciences, Sanandaj, Iran. ²Department of Environmental Health Engineering, Faculty of Health, Kurdistan University of Medical Sciences, Sanandaj, Iran. ³Department of Environmental Health Engineering, School of Health, Arak University of Medical Sciences, Arak, Iran. ⁴Department of Environmental Health Engineering, School of Public Health, Khoy University of Medical Sciences, Khoy, Iran. ✉email: esrafil_asgari@khoyums.ac.ir

carbon, clay, natural zeolite, furnace ash, bentonite, polymers, resin, biological absorbents, and hazelnut shells have been used to remove heavy metals from aqueous environments^{13,14}. Silica materials are considered as desirable adsorbents because of the ability of their surface functional groups in the adsorption of target pollutants^{15,16}. Diatomaceous earth, also called biological silica (biosilica), is a siliceous sedimentary rock containing more than 90% silicon dioxide. Because of the presence of active surface groups on high surface area, biological silica is considered as a suitable adsorbent for the adsorption of various organic and inorganic pollutants from wastewater^{17,18}. Among different synthetic adsorbents, nano-sized adsorbents have gained much attention due to their fine size and consequently large surface areas for the efficient adsorption of target pollutants^{19,20}. Magnetite nanoparticles are proposed as common adsorbent owing to their large specific surface area and ease of synthesis to be used as individual adsorbent or in combination with other adsorbents^{1,7,14}. In addition, easy separation of magnetite nanoparticles by an external magnetic field is the main advantage of this adsorbent. However, the adsorption capacity of nanoparticles and their selectivity are not satisfactory as well as their stability in acidic conditions^{21,22}.

The separation and recycling of the adsorbent are of important problems during the implementation of nanostructured adsorbents. Thus, the immobilization of nanoparticles within a suitable matrix is proposed as an effective approach to enhance reusability potential of the adsorbent. Polymeric substances such as alginate and chitosan are the most extensively used compounds to immobilize nanostructured adsorbents. Among polymeric substances, alginate is attracted more attentions among researchers because of its high reactivity, low cost and high adsorption capacity²³. Environmentally, alginate is nontoxic with high biodegradability²⁴. Therefore, it can be widely used as a gel matrix, membrane material, and water-blocking agent. Due to its high quantities of carbonyl groups and oxygen atoms, alginate is an efficient adsorbent for metal ions²⁴. Therefore, the current study focused on the preparation of magnetite (Fe₃O₄)@biosilica/alginate (MBA) nano-hybrid and its application for the adsorption of cadmium ions from aqueous environments. Dual immobilization of magnetite nanoparticles and biosilica was considered to avoid the washout of fine particles from the liquid phase. This approach was utilized to not only effectively immobilize nanostructured adsorbents but also improve the adsorption capacity of the immobilized components. In addition to high adsorption capacity, the aforementioned nanostructured adsorbents can be removed from the solution and being recycled by an external magnetic field.

Materials and experimental procedure

Materials. Diatomaceous earth (~97.5% SiO₂ basis) and sodium alginate (C₆H₉NaO₇) were purchased from Sigma Aldrich Company. Cadmium nitrate (Cd(NO₃)₂) and other chemicals were provided by Merck Co. (Germany). The chemicals used in the current study were reagent and laboratory grade and utilized without any changes.

Preparation of nano-adsorbents. *Preparation of magnetic biosilica.* In the current study, the common chemical precipitation method by FeCl₂·4H₂O, FeCl₃·6H₂O, and biosilica were added to ammonia solution under nitrogen gas flow to prepare magnetic biosilica via a simple chemical precipitation method. Firstly, 2.0 g of biosilica was added to the distilled water (100 mL) and placed in an ultrasonic bath for 12 h to attain a homogeneous mixture with weigh percent of 2%. Also, 0.8457 g of iron chloride (II) and 2.2992 g of iron chloride (III) were dissolved in distilled water (50 mL). In the following, 50 mL of the biosilica mixture was added to 50 mL of iron chloride solutions and stirred for 30 min under nitrogen gas flow of 80 °C. Then, 25 mL of 25% ammonia (w/w) was injected into the stirring mixture under nitrogen gas flow for a further 1.0 h. In the next step, the magnetic biosilica was collected using a Block Neodymium Magnet and washed with ethanol and distilled water repeatedly. Finally, as-synthesized magnetic biosilica was dried in an oven at 70 °C²⁵.

Preparation of MBA nano-hybrid. To prepare the MBA nano-hybrid, 1.0 g of sodium alginate (C₆H₉NaO₇) was added to 100 mL of acetic acid 1.0 M and mixed. Then, 1.0 g of magnetic biosilica was also added to acetic acid and sodium alginate solution, and then mixed until obtaining a homogenous viscous solution. The mixture was subsequently provided in a final volume of 100 mL (4.0:1.0 ratio for 15% NaOH to 95% ethanol). The viscous mixture of sodium alginate, alginate/magnetic biosilica was dropped into NaOH/ethanol using a syringe. The bullet-shaped compounds formed in this stage were set aside for 24 h. The beads obtained from nano-hybrid were washed with the pure water until reaching neutral pH then dried at room temperature. Finally, the dried beads were crushed in mortar and graded using a standard sieve²⁶.

Experimental procedure. In the current study, all the experiments were done in batch flow mode reactors using 100-mL glass Erlenmeyers. Also, the effect of the main parameters of solution pH (2.0–9.0), contact time (10–180 min), MBA nano-hybrid dosage (0.25–4.0 g/L), cadmium concentration (10–320 mg/L), and temperature (25–55 °C) on the adsorption process of Cd(II) ions were assessed. For preparation of stock solution (1000 mg/L of Cd), double distilled water was used. The solution pH was adjusted using either 0.1 M NaOH or 0.1 M H₂SO₄. The certain concentrations of cadmium (50.00 mL) were prepared and the desired changes were applied to each Erlenmeyer. The batch reactors were then placed on a shaker (150 rpm) to mix and carry out the adsorption process. After the completion of the process, Cd-contained samples were taken from the reactor at regular time intervals and analyzed. The kinetics studies, isotherm models, thermodynamics, recovery of nano-hybrid and the effect of other cations (Na⁺, K⁺, Mg²⁺ and Ca²⁺) on the adsorption of Cd(II) were also studied. The experiments were performed thrice and the mean values were recorded. The adsorption efficiency of Cd(II) ions was calculated according to Eq. (1), in which C₀ and C_e are the initial concentration and equilibrium concentrations of Cd(II) ion (mg/L), respectively:

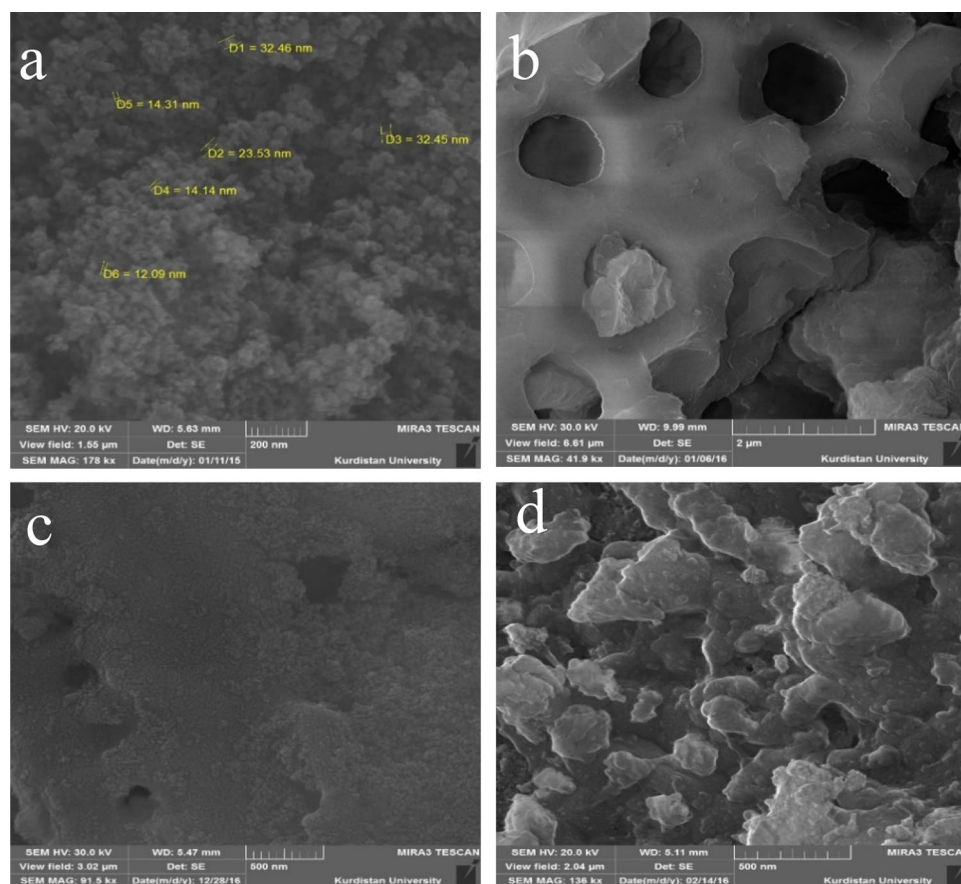


Figure 1. SEM images of nano-sized Fe_3O_4 (a), biosilica (b), biosilica/ Fe_3O_4 (c) and MBA nano-hybrid (d).

$$\% \text{Removal} = \frac{C_0 - C_e}{C_e} \times 100 \quad (1)$$

The quantity of Cd(II) ions adsorbed onto the nano-hybrid in equilibrium at time t (min) was determined Eq. (2)²⁷:

$$q_t = \frac{(C_0 - C_t)V}{W}. \quad (2)$$

Analyses. The Fourier transform infrared spectroscopy (FT-IR), scanning electron microscopy (SEM), and X-ray diffraction (XRD) techniques were used to identify and characterize the nano-hybrid. The morphology of the nano-hybrid was investigated with SEM (Model: MIRA III, TESCAN, Czech Republic). The crystalline structure of nano-hybrid was examined using a XRD apparatus (Model: PW-1730, Philips, the Netherlands). Additionally, the surface functional groups of the nano-hybrid were determined using the FT-IR spectroscopy (Model: AVATAR, Thermo, USA). For this analysis, the KBr pellet was prepared using specific amount of the powder sample. Then, as-prepared pellet was used in the instrument to obtain the spectrum in the wavenumber range of $500\text{--}4000\text{ cm}^{-1}$.

The cadmium amount was measured in the samples before and after the adsorption process using atomic adsorption spectrometry (AAS, Model: AA-7000, Shimadzu, Japan)².

Consent for publication. All the authors agree to publish this article.

Results and discussion

Nano-hybrid characterization. Figure 1 shows SEM images of the synthesized nano-hybrid. Comparing the SEM images shows significant change in the morphology of the nano-hybrid after the immobilization.

Figure 1a shows surface morphology of the magnetite particles. As shown, magnetite particles are formed in nano-size during the synthesis procedure. Porous structure of biosilica can be observed in Fig. 1b, indicating its suitability to be used as support for the magnetite nanoparticles. Figure 1c shows that magnetite nanoparticles are distributed on the biosilica surface. Biosilica surface is covered by ultrafine particles of magnetite. Figure 1d displays biosilica/magnetite immobilized into alginate matrix. The appropriate entrapment of biosilica/magnetite

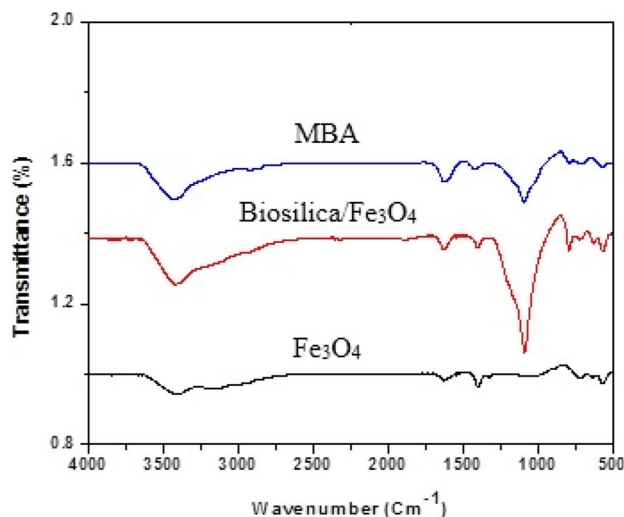


Figure 2. FT-IR spectra of Fe_3O_4 , biosilica/ Fe_3O_4 and MBA nano-hybrid.

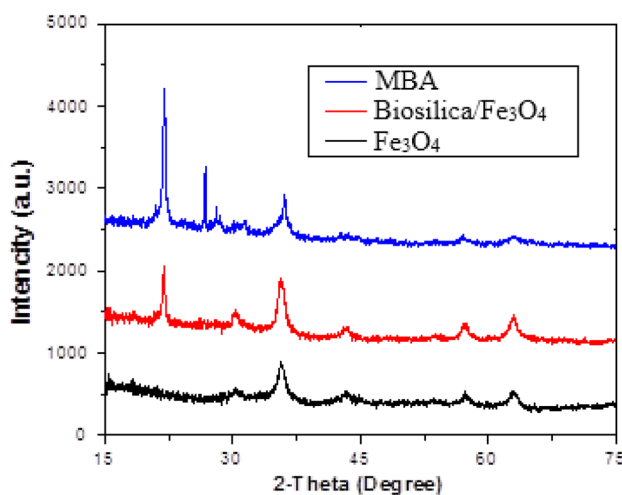


Figure 3. The XRD pattern of Fe_3O_4 , biosilica/ Fe_3O_4 and MBA nano-hybrid.

in the alginate matrix is obvious. However, the nano-hybrid has suitable porous structure containing biosilica and especially magnetite nanoparticles exposed to the target pollutant ions for the efficient adsorption.

Although the size of the nano-hybrid increased in comparison with the composing nanostructured components but such combination, as explained in the adsorption experiments section, resulted in the enhanced adsorption of Cd ions. On the other hand, the nature of the MBA nano-hybrid makes it a superior adsorbent for the adsorption of heavy metal ions such as Cd.

The effect of adding biosilica and alginate on the functional groups of Fe_3O_4 was studied using the FT-IR analysis. Figure 2 presents the spectra of Fe_3O_4 , Biosilica/ Fe_3O_4 and MBA nano-hybrid. A new peak placed at 1200 cm^{-1} (symmetric stretching mode of Si–O–Si bond) reveals the presence of biosilica in the structure of biosilica/ Fe_3O_4 ; however, the intensity of biosilica characteristic peak was reduced due to the presence of alginate in the nano-hybrid. Moreover, the peak located at wavenumber of 800 cm^{-1} represents stretching Si–O group of the biosilica structure¹⁶. The weak peak placed around 570 cm^{-1} indicates the presence of Fe_3O_4 .

The peak around 3400 cm^{-1} may be associated with the stretching vibration of OH group, which intensified after the immobilization of Fe_3O_4 nanoparticles, indicating the involvement of hydroxyl group in the immobilization of Fe_3O_4 nanoparticles²⁶.

The crystalline structure of the nano-hybrid was analyzed using XRD analysis. The patterns are provided in Fig. 3. It is obvious that the combination of biosilica with Fe_3O_4 resulted in appearing new peak at 21.9° . It is in accordance with the JCPDS Card number of 00–001–0647 which is associated with the pure silica structure²⁸. The third pattern (MBA) confirmed crystalline nature of the nano-hybrid even after the immobilization via amorphous alginate polymeric matrix²⁹.

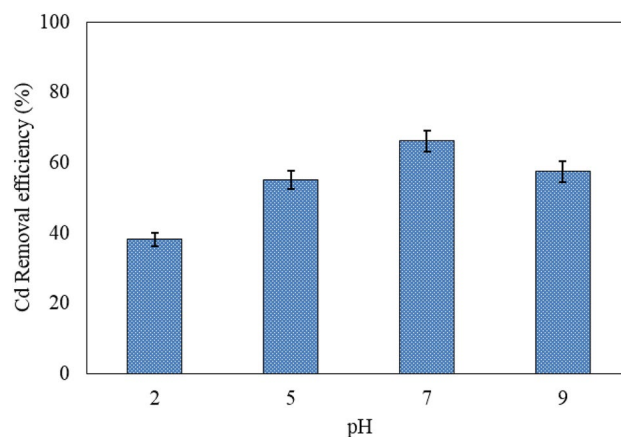


Figure 4. Effect of pH on the adsorption of Cd on MBA nano-hybrid. ($[Cd]_0 = 40$ mg/L, $[MBA]_0 = 1.0$ g/L, temperature = 25 °C, contact time = 60 min).

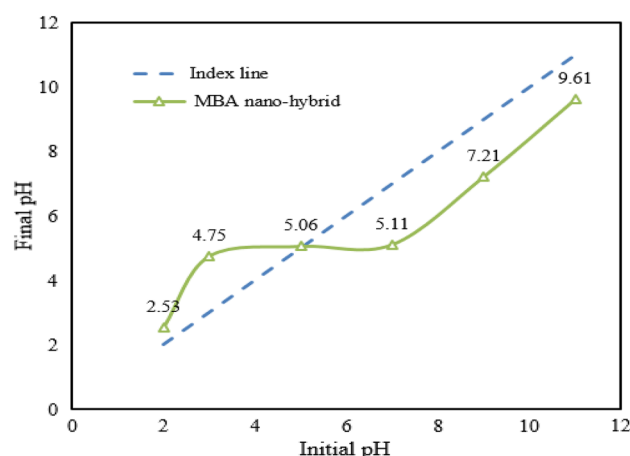


Figure 5. pH_{zpc} of MBA nano-hybrid.

Moreover, intensity of the peak located at 30° increased, which demonstrated the appropriate incorporation of Fe_3O_4 into the biosilica structure. On the other hand, alginate biopolymer not only resulted in appearing a new peak at 25° but also slightly displaced the biosilica peak. It indicated the enlargement of the basal spacing of the biosilica due to the interactions between biosilica and alginate²⁹. The XRD patterns confirmed the presence of alginate, biosilica and Fe_3O_4 in an integrated lattice.

Effect of experimental parameters. *Effect of solution pH.* The adsorption of target pollutants especially heavy metal ions on a hybrid adsorbent such as MBA nano-hybrid usually depends on the initial pH of the solution³⁰. The hydrolysis and deposition properties of metal ion species are influenced by the solution pH³¹. In this study, the effect of initial pH on the adsorption of Cd ions was investigated at the initial Cd concentration of 40 mg/L, nano-hybrid dosage of 1.0 g/L, temperature of 25 °C, stirring rate of 150 rpm and contact time of 60 min (Fig. 4).

The MBA nano-hybrid showed less affinity to Cd ions at strong acidic conditions. The alginate in the structure of MBA nano-hybrid contains large amounts of polysaccharides, some of which are linked to proteins and other components. These macromolecules on the surface of the alginate have several surface functional groups such as carboxyl, thiol, amine, and phosphate³¹.

The efficiency of Cd adsorption depends on the protonation and deprotonation of the surface functional groups of the nano-hybrid surface. The nano-hybrid electric charge and ionic forms of Cd ions depend on solution pH. To understand the type and amount of the surface charge of the studied MBA nano-hybrid at different pHs, pH_{zpc} value of the nano-hybrid was measured. Based on the result, pH_{zpc} value of about 5.06 was obtained. Therefore, the surface charge of the nano-hybrid was negative at pH values above 5.06. At $pH < pH_{zpc}$, the surface charge was positive (Fig. 5).

The highest adsorption efficiency of Cd ions was obtained at the initial pH of 7.0. Increasing the initial pH from 7.0 to 9.0 led to a 9.0% reduction in the removal efficiency of Cd ions. In fact, the gravity force between the positive Cd ions and the MBA nano-hybrid reached the highest at pH values above 5.0. The lowest Cd removal

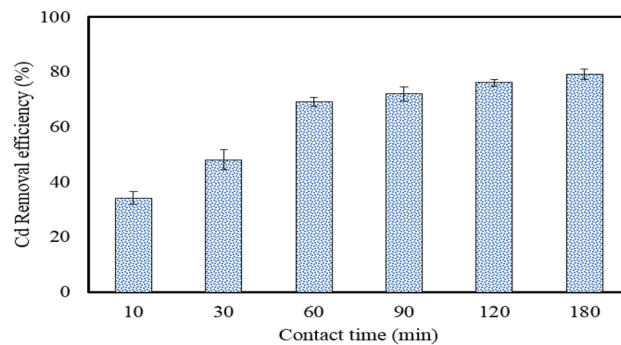


Figure 6. The effect of adsorption time on the removal of Cd by the MBA nano-hybrid. ($[Cd]_0 = 40$ mg/L, pH = 7.0, adsorbent = 1.0 g/L, temperature = 25 °C).

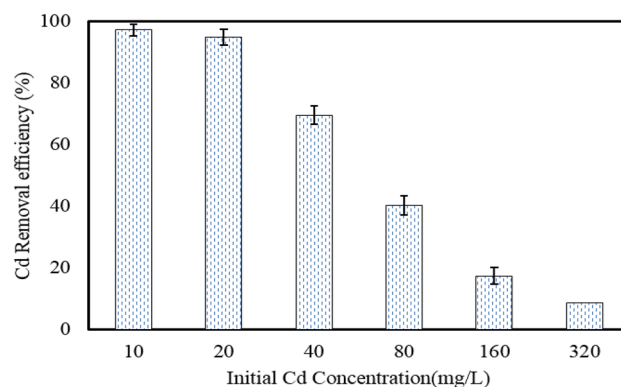


Figure 7. The effect of initial concentration of Cd on its removal by the MBA nano-hybrid (pH = 7.0, adsorbent = 1.0 g/L, temperature = 25 °C, time = 60 min).

value was observed at pH 2.0, which is due to the competition between Cd ions and H⁺ ions for occupying adsorptive sites of the nano-hybrid.

In addition, the results of other studies show that in most cases, maximum Cd removal occurred in the pH range of 4.0–7.0 (weak acidic and neutral), which is in accordance with the results of the present study³². Maximum Cd removal occurred in the studies of Bayramoglu et al. in pH 6.0³¹, Alakhras in pH 5.0³³, Dolgormaa et al. in pH 5.0³⁴ and Shen et al. in pH 6.0³².

Effect of contact time. After determining the optimum pH, the effect of contact time on the removal of Cd by the MBA nano-hybrid was investigated at the initial Cd concentration of 40 mg/L, adsorbent dose of 1.0 g/L and temperature of 25 °C within the contact time of 180 min. As shown in Fig. 6, the increase in contact time promoted Cd removal efficiency. The removal efficiency of Cd increased from 34.20 to 79.23% by increasing the contact time from 10 to 180 min, respectively.

At the beginning of the adsorption process, the removal efficiency was fast, reaching 69.17% and then almost reached a plateau at later times. The major reason for this behavior is the saturation of the active sites in the nano-hybrid, which do not allow for further adsorption. This can be explained by the fact that initially the number of sites on the surface of the nano-hybrid is very high, which makes adsorption very fast, but over time, the active sites become saturated, hence reducing adsorption rate³⁵.

Effect of initial Cd concentration. As displayed in Fig. 7, it is observed that increasing the initial Cd concentration results in the decreased removal efficiency of Cd by the nano-hybrid. As can be seen in Fig. 7, the removal efficiency decreased from 97.3 to 8.57% with increasing the concentration of Cd from 10 to 320 mg/L, respectively. At the initial Cd concentration of 40 mg/L, the removal efficiency was 69.57%.

As the adsorption sites are constant for a certain amount of nano-hybrid, the removal efficiency of Cd(II) decreases with increasing the Cd(II) concentration. The decrease in the ratio of Cd(II) residue to initial concentration of Cd(II) by increasing the initial concentration of Cd(II) can also be ascribed to the enhancement in the driving force due to an increase in the initial Cd(II) concentration, which is caused by the repulsive forces between Cd(II) and prevention of adsorption of Cd(II) on the nano-hybrid.

A study by Benhima et al.³⁶ on the removal of both Cd(II) and Pb ions from aqueous solution via the adsorption on microparticles of dry plants and another study by Wang et al.³⁷ on the removal of Cd (II) by crude clay

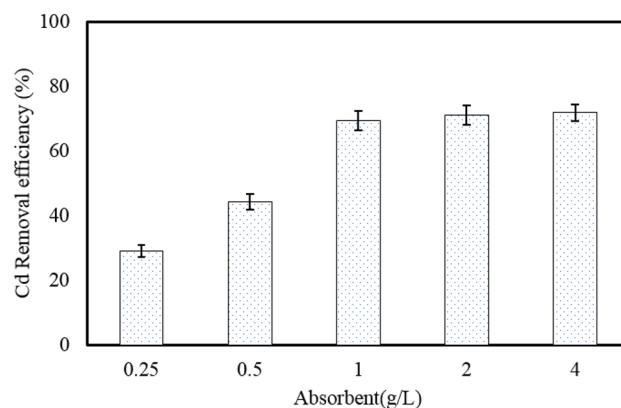


Figure 8. The effect of dosage of adsorbent on the removal efficiency of Cd(II) by MBA nano-hybrid ($C_0 = 40$ mg/L, pH = 7.0, temperature = 25 °C, time = 60 min).

(raw attapulgite clay) from aqueous solution have shown the decreased removal efficiency by increasing the initial concentration of the target pollutants. This finding could be due to the number of fixed sites on a given amount of adsorbent.

Effect of adsorbent dosage. As can be noted in Fig. 8, Cd removal efficiency increases with increasing dosage of nano-hybrid. Increasing the adsorbent dosage from 0.25 to 1.0 g/L improved the adsorption efficiency of Cd(II) ions from 29.1 to 69.3%, respectively. Also, increasing the nano-hybrid dosage from 2.0 to 4.0 g/L had no significant effect on Cd(II) ion removal efficiency and resulted in a very slight increase in the efficiency from 71.1 to 71.8%, respectively. It is clear that as the amount of adsorbent increases, the number of available adsorption sites increases, so the adsorption efficiency improves, but the adsorption rate which is the amount of pollutant adsorbed per mass unit of the adsorbent (mg/g), diminished. Therefore, the adsorbent dosage of 1.0 g/L was selected as the optimal dosage for performing the rest of experiments^{35,37}.

Kinetic study. The prediction of the adsorption process is one of the major factors during designing an adsorption system³⁸. Four different kinetic models including pseudo-first-order, pseudo-second order, intra-particle diffusion and Elovich models (Eqs. (3) to (6)) were used to investigate the kinetic of Cd adsorption on the MBA nano-hybrid at an initial concentration of 40 mg/L.

The pseudo-first and pseudo-second order kinetic models are expressed in the Eqs. (3) to (4)^{30,39}:

$$\ln(q_e - q_t) = \ln q_e - k_1 t \quad (3)$$

$$\frac{t}{q_t} = \frac{1}{k_2 q_e^2} + \frac{t}{q_e} \quad (4)$$

where q_t and q_e (mg/g) are the values of adsorbed cadmium at t and equilibrium time, respectively. K_1 (1/min) and K_2 (g/(mg.min)) are the rate constants of the first- and second-order models, respectively.

The intra-particle diffusion model (Eq. (5)) was also used to characterize the multi-step and competitive adsorptions in the adsorption process, and the Elovich model (Eq. (6)), based on the adsorption capacity, was employed to describe the kinetics of chemical adsorption⁴⁰.

$$q_t = k_{int} t^{1/2} + C \quad (5)$$

where K_{int} is the intra-particle infiltration rate constant in mg.min^{1/2}/g, C is the intra-particle infiltration constant in mg/g and q_t is as previously defined.

$$q_t = \frac{1}{\beta} \ln(\alpha\beta) + \frac{1}{\beta} \ln t \quad (6)$$

where α is the initial adsorption rate as mg/g.min, and β is the surface coverage (desorption) as g/mg. In the Elovich equation, the values of α and β parameters was obtained by plotting q_t against $\ln t$.

The results of kinetic study are summarized in Table 1 and Fig. 9. Table 1 shows that the pseudo-second-order kinetic model with the correlation coefficient of 0.99 is the most suitable kinetic model to describe the adsorption process and the calculated adsorption capacity (q_{cal}) is completely consistent with the experimental data (q_{exp}).

Given the low regression coefficients of the pseudo-first-order kinetic models, intra-particle diffusion and Elovich models with the regression coefficients of 0.85, 0.89 and 0.85, respectively, these models cannot describe the Cd adsorption process on the MBA nano-hybrid well and the mentioned adsorption system does not follow these models. Therefore, the pseudo-second-order kinetic model is more suitable for the Cd adsorption process on the MBA nano-hybrid. Badruddoza et al. in their study of heavy metal removal with Fe₃O₄/cyclodextrin

Kinetic models	Kinetic parameters	Values at $C_0 = 40$ mg/L
Pseudo-first order	q_{exp} (mg/g)	35.38
	q_e (mg/g)	22.16
	K_1 (1/min)	0.0067
	r^2	0.8518
Pseudo-second order	q_e (mg/g)	35.44
	K_2 (g/(mg.min))	0.12
	r^2	0.9972
Intra-particle	C (mg/g)	0.5
	K_{int} (mg/g.min)	0.091
	r^2	0.89
Elovich	α (mg/g.min)	27.5
	β (g/mg)	0.59
	r^2	0.85

Table 1. Kinetic parameters for the removal of Cd by the MBA nano-hybrid. (pH = 7.0, $[MBA]_0 = 1.0$ g/L, temperature = 25 °C, contact time = 60 min).

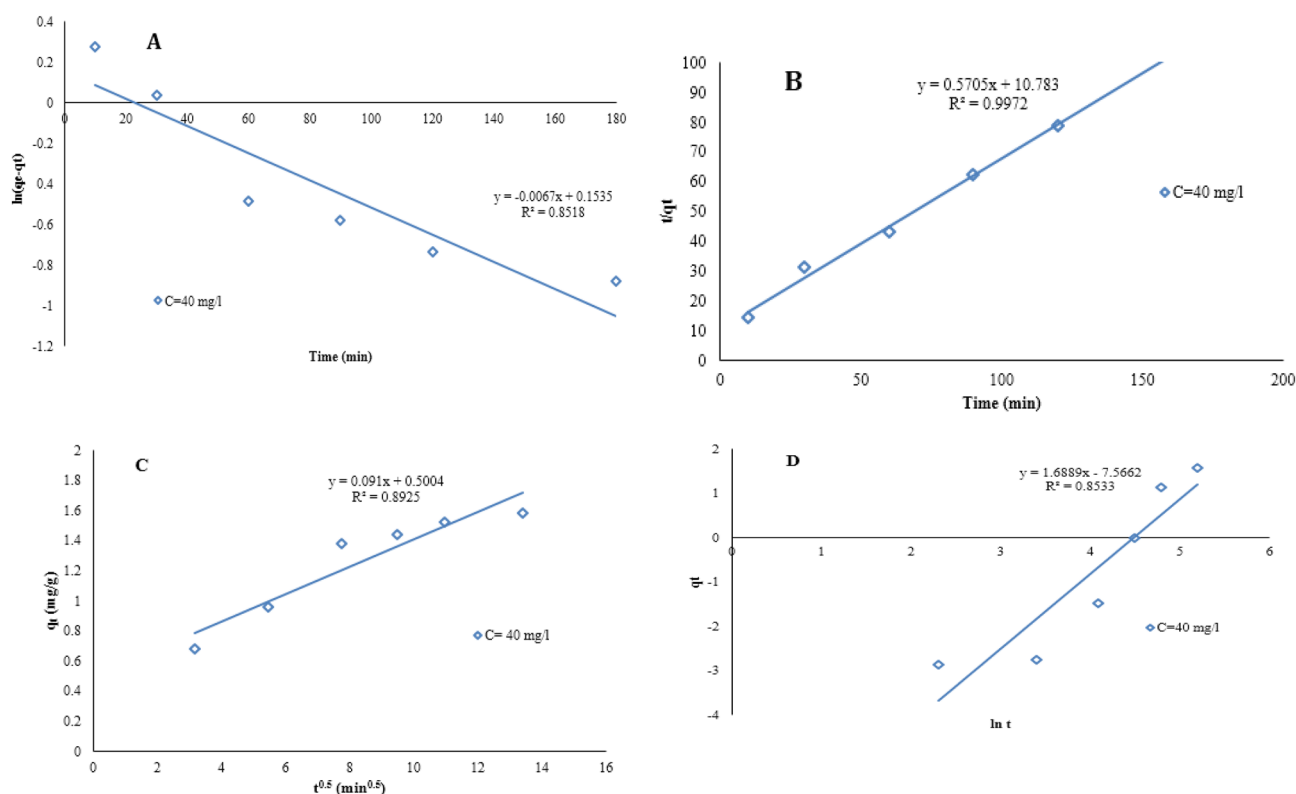


Figure 9. The kinetic models for the removal of Cd by MBA nano-hybrid: (a) Pseudo-first order, (b) Pseudo-second order, (c) Intra-particle (d) and Elovich models (pH = 7.0, adsorbent = 1.0 g/L, temperature = 25 °C, optimum time = 60 min).

polymeric nanocomposite showed the highest agreement with the pseudo-second-order model and the regression coefficient was above 99%⁴¹. The results of the present study are also in agreement with those of Yi et al.^{42,43}.

Isotherms study. Adsorption isotherm shows how the heavy metal ions are distributed between the liquid phase and the solid phase at the equilibrium state⁴². To further elucidate the mechanism of Cd(II) adsorption, Langmuir, Freundlich, and Temkin isotherm models were used [Eqs. (7) to (9)]^{27,44,45}.

$$q_e = \frac{q_m K_L C_e}{1 + K_L C_e} \quad (7)$$

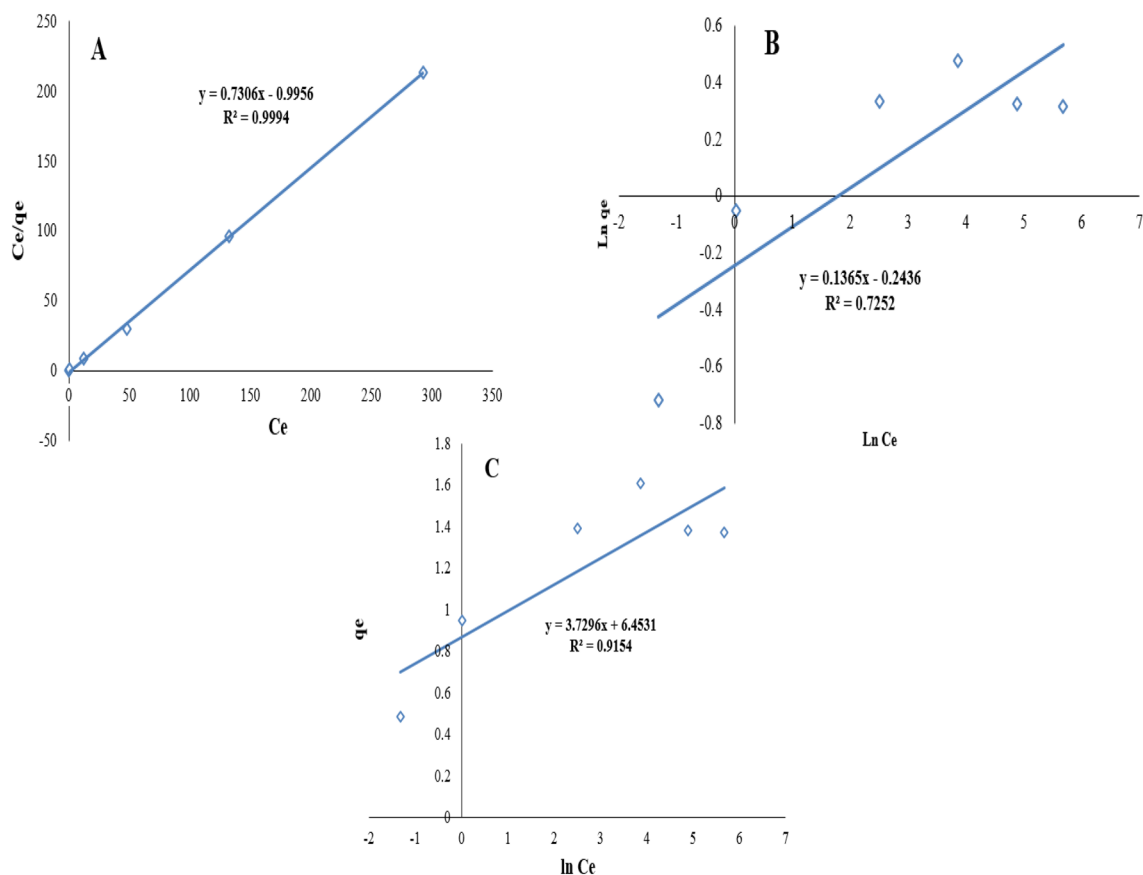


Figure 10. Adsorption isotherms for the removal of Cd by the MBA nano-hybrid: (a) Langmuir, (b) Freundlich and (c) Temkin (pH = 7.0, adsorbent = 1.0 g/L, temperature = 25 °C, optimum time = 60 min).

Isotherm equation	Kinetic parameters	Values
Langmuir	q_m (mg/g)	35.36
	b	0.73
	R_L	0.026
	r^2	0.99
Freundlich	n	7.32
	K_F (mg/g(L/mg) ^{1/n})	1.27
	r^2	0.72
Temkin	A	3.72
	B	6.45
	r^2	0.91

Table 2. Isotherm modeling parameters for the removal of Cd by the MBA nano-hybrid: (a) Langmuir, (b) Freundlich (c) and Temkin. (pH = 7.0, adsorbent = 1.0 g/L, temperature = 25 °C, optimum time = 60 min).

$$q_e = K_F c_e^{\frac{1}{n}} \quad (8)$$

$$q_e = B \ln K_t + B \ln c_e \quad (9)$$

In these equations, C_e is the equilibrium concentration of the adsorbed material (mg/L), q_e is the adsorption capacity at equilibrium (mg/g), q_m is the maximum adsorption capacity (mg/g), K_L is the Langmuir equilibrium constant (L/mg). In the Freundlich isotherm model, K_F is the Freundlich constant (mg/g) and $1/n$ is the absorption intensity. In the Temkin isotherm model, B is the isotherm constant (J/mol) and A is the binding constant of Temkin (L/g)⁴⁴.

The isothermal curves constructed with the Langmuir, Freundlich, and Temkin correspond to a, b, and c in Fig. 10, respectively. Table 2 summarizes the calculated isothermal parameters. According to the results of Table 2, the maximum Cd(II) adsorption is approximately 35.36 mg/g at 25 °C. Compared with the Temkin and

Adsorbent type	q_m (mg/g)	pH	Isotherm	Temperature (°K)	References
Attapulgit	10.38	5.45	L	298	37
Porous resin	3.51	7.0	L	298	49
Aluminum hydroxide modified steel-making slag	10.16	4.0	L	298	50
Montmorillonite	15.09	5.0	F	303	51
wheat straw	0.13	7.0	L	298	52
Bamboo charcoal	12.08	≥ 8.0	L	298	53
Modified sewage sludge	14.7	7.0	L	298	54
Bentonite	9.30	7.0	L	298	55
MBA nano-hybrid	35.36	7.0	L	298	This study

Table 3. Adsorption of Cd(II) ions from aqueous solutions by different adsorbents.

Freundlich models, the Langmuir isotherm model with R^2 value of higher than 0.99 is more suitable for describing adsorption data of the Cd(II) adsorption on the MBA nano-hybrid.

This result indicates uniform distribution of active sites on the MBA nano-hybrid surface, resulting in the single-layer adsorption of Cd(II) at homogeneous sites. Also, the adsorption of materials from the liquid phase onto the synthesized nano-hybrid is monolayer and the energy is the same during the adsorption process⁴². Also, in the Liu et al. study, which was performed to remove Cadmium, lead and copper ions from aqueous media, the results showed that the Langmuir model had a high regression coefficient compared with the Freundlich isotherm⁴⁶. In the Badruddoza study, it was found that the adsorption data are more in line with the Langmuir isotherm, which is consistent with the results obtained from the present study⁴¹.

In addition, for further analysis of the Langmuir model, the dimensionless partition coefficient (R_L) can be used (Eq. (10)), which is designed to evaluate the degree of adsorption desirability⁷. $R_L > 1$ indicates non-desirable type of adsorption, $R_L = 1$ shows linear adsorption, and $0 < R_L < 1$ demonstrates a desirable adsorption and an irreversible adsorption^{47,48}.

$$R_L = \frac{1}{1 + K_L c_0} \quad (10)$$

The R_L value for the present study at 25 °C is 0.026, indicating an optimum adsorption of Cd(II) molecules on the MBA nano-hybrid. In the Freundlich model, on the other hand, the value of n is within the range of 1–10, indicating the desired adsorbent adsorption on the adsorbent⁷.

Table 3 compares the maximum adsorption capacity (q_m) of the MBA nano-hybrid for the adsorption of Cd(II) ions with other previously reported adsorbents. The data tabulated in Table 3 shows that the q_m of Cd(II) ions onto MBA nano-hybrid is higher than some of other adsorbents. The q_m value of MBA nano-hybrid adsorbing Cd(II) was higher than some of other adsorbents, and MBA could be recovered by a magnetic field, indicating that the adsorbent can be possibly applied for the removal of Cd(II) from aqueous solutions.

Effect of coexisting cations. The simulated test aqueous solution in this study does not contain other ions, while metal cations such as Ca^{2+} , Mg^{2+} , Na^+ and K^+ are very common in natural waters or actual wastewater and easily exhibit competitive adsorption with the target heavy metal ions⁵⁶. In this study, the adsorption efficiency of Cd(II) ions on the MBA nano-hybrid was determined in the presence of four metal cations at two concentrations of 40 and 80 mg/L. As can be seen in Fig. 11, an increase in the concentration of metal cation ions from 40 to 80 mg/L results in a drop in Cd(II) removal efficiency.

The reduction in Cd(II) ions removal efficiency with the increasing the concentration of monovalent ions (Na^+ and K^+) had a slight inhibitory effect on the adsorption of Cd(II) ions, such that at a concentration of 80 mg/L in the presence of sodium and potassium ions, the removal efficiency dropped to 51 through 50% from 69.17% for the non-ionic increase. This is while the decrease in efficiency in increasing the concentration of divalent ions (Mg^{2+} and Ca^{2+}) had a higher inhibitory effect on the adsorption of Cd(II) ions, such that at the 80 mg/L concentration in the presence of calcium and magnesium ions, the removal efficiency reduced to 42% through 38% from 69.17% for non-ionic enhancement. The greater effect of Ca^{2+} on Cd(II) adsorption is because of more similar ion radii of Ca^{2+} with Cd^{2+} than Mg^{2+} (ion radius are 0.99, 0.97 and 0.65 Å for Ca^{2+} with Cd(II) and Mg^{2+} respectively). On the other hand, Ca^{2+} can form complexes with water molecules, $Ca^{2+}-(H_2O)_n$, that covering surface of adsorbent which resulting decreased availability of active sites on the adsorbent. It can be expected, $Ca^{2+}-(H_2O)_n$ with larger radius than $Mg^{2+}-(H_2O)_n$ has bigger steric hindrance and so its negative effect on adsorption is stronger^{57,58}. Since concentration of Ca^{2+} and Mg^{2+} in fresh water is approximately between 10 and 80 mg/L, so the presence of these cations with these levels of concentration have not significant effect on Cd(II) adsorption.

Thermodynamic study. Solution temperature affects the rate of adsorption⁵⁹. According to Arrhenius, absorption rate usually elevates with increasing temperature and reduces with decreasing temperature³³. Such observation could be attributed to the increase in the size of the pores on the adsorbent surface or the increase in effective collisions between the adsorptive and the adsorbent⁶⁰.

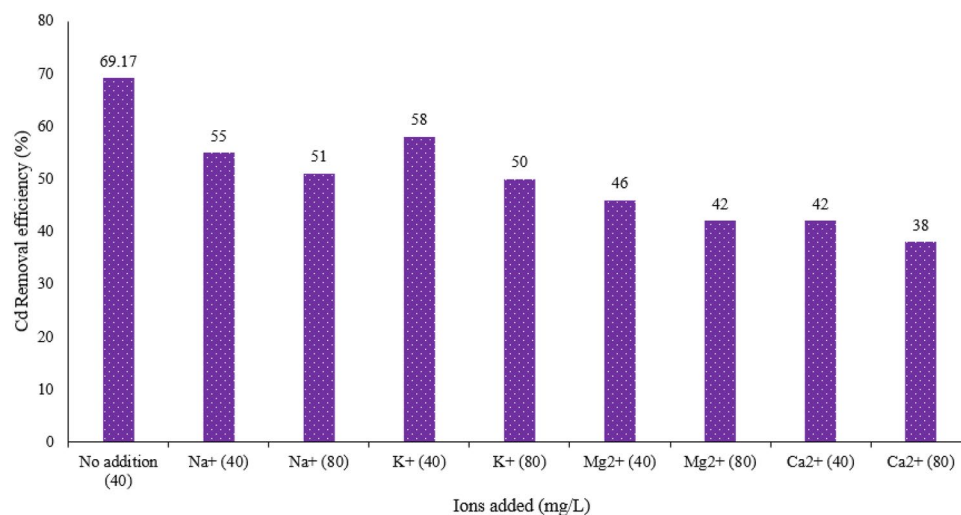


Figure 11. Effect of sodium, potassium, magnesium and calcium ions on the removal of Cd(II) by the MBA nano-hybrid (pH = 7.0, adsorbent = 1.0 g/L, temperature = 25 °C, time = 60 min).

Concentration (mg/L)	ΔH° (kJ/mol)				ΔG° (kJ/mol)	ΔS° (kJ/K.mol)
	298 °k	308 °k	318 °k	318 °k		
40	-8.13	-7.16	-6.06	-5.54	88.21	-20.88

Table 4. Thermodynamic parameters for Cd(II) removal by the MBA nano-hybrid (pH = 7.0, adsorbent = 1.0 g/L, temperature = 25 °C, time = 60 min).

The adsorption mechanism for the Cd(II) adsorption on the MBA nano-hybrid is investigated by the thermodynamic parameters such as changes in enthalpy ΔH° (kJ/mol), entropy ΔS° (kJ/K.mol) and Gibbs free energy ΔG° (kJ/mol) based on the equations presented below [Eqs. (11)–(13)].

$$\Delta G^\circ = -RT(\ln K_c) \quad (11)$$

$$\ln k_c = \Delta S^\circ / R - \Delta H^\circ / RT \quad (12)$$

$$k_c = q_e / C_e \quad (13)$$

where T (°K) is the temperature, R (8.314 J/mol.K) is the global gas constant and K_c (L/g) is the ratio of the adsorbed material to the adsorbent remaining in the solution (mg/g).

The results of the thermodynamic study of the adsorption of Cd by the MBA nano-hybrid are presented in Table 4. As shown, the numerical value of ΔH° was obtained to be negative, indicating that the adsorption process is exothermic. In other words, the increase in temperature has a negative effect on the adsorption of Cd(II) and, the adsorption of this pollutant at lower temperatures is more favorable. The ΔS° parameter was positive in this process, showing an increase in the irregularity with increasing temperature in the solid–liquid phase during the adsorption process. A negative ΔG° also means that the adsorption process of Cd(II) on the adsorbent is feasible and thermodynamically spontaneous. These results are in agreement with the findings of Witek-Krowiak during the adsorption of heavy metals from aqueous solutions using beech wood sawdust⁶¹.

Adsorbent reusability. To investigate the reusability of adsorbent, MBA nano-hybrids were separated using an external magnetic field at the end of each adsorption run. Then, MBA nano-hybrids were placed into 20 mL of HCl (0.1 M) or NaOH (0.1 M) aqueous solutions as desorption solutions for 4.0 h, and washed three times with half-liter of D.I water to remove unadsorbed traces of Cd(II) ions. The washed and recovered adsorbent was dried at 60 °C for 24 h in an oven and reused in further adsorption cycles⁶². According to the results, the Cd(II) removal efficiency by the MBA nano-hybrid decreased from 69.17 to 52.6% within five adsorption cycles (Fig. 12). In other words, the MBA nano-hybrid can be recycled and reused for up to five consecutive times with the adsorption efficiency above 52.6%. According to the results, the desorption rate of HCl was higher than NaOH at all stages. When HCl was used as the desorption solution, the desorption percentage was greater than 52.1% for the Cd(II) adsorbed on the MBA nano-hybrid in the first stage and more than 30.1% at the end of fifth stage.

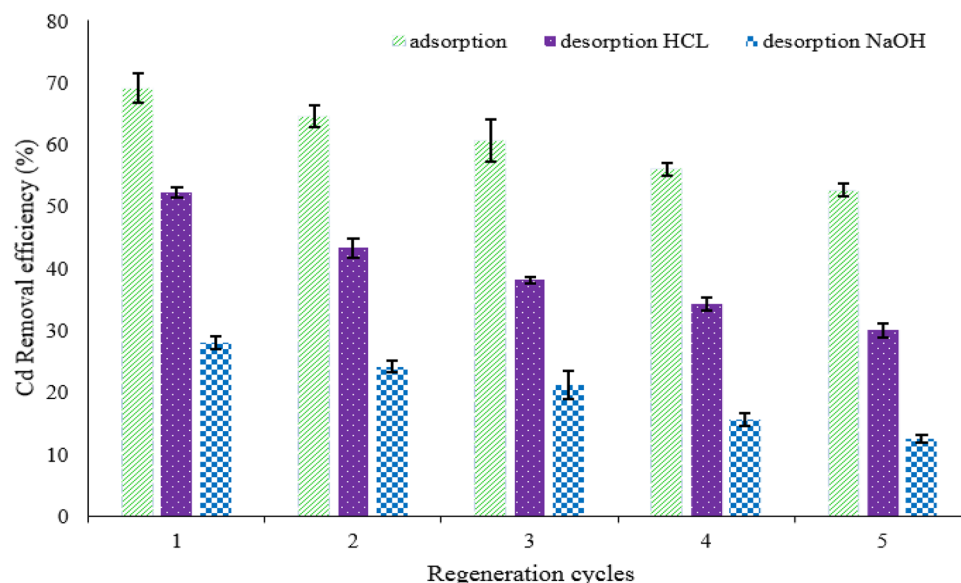


Figure 12. The removal efficiency of Cd(II) on fresh & regenerated MBA nano-hybrid with using HCL & NaOH. (pH = 7.0, adsorbent = 1.0 g/L, temperature = 25 °C, time = 60 min).

However, when NaOH was used as the desorption solution, the desorption rate was 28% for the adsorbed Cd(II) on the MBA nano-hybrid in the first stage and more than 12.5% in the fifth stage. The high amount of desorption using HCl can be attributed to the protonation of the adsorbent surface by the use of acidic agents. According to the Cechinel et al. study, HCl covers the surface of the adsorbent using H^+ protons and completely protonates the adsorbent for the next stage⁶³. The results of the present study are also in agreement with those of Yi et al.^{42,43}.

Conclusion

In summary, the MBA nano-hybrid was synthesized and characterized for the adsorption of cadmium ion as target pollutant in the aquatic environment. According to the results, MBA nano-hybrid were successfully utilized for the adsorption of Cd(II) ions from aqueous solution. Moreover, the adsorption of Cd(II) ions onto the nano-hybrid was pH-dependent. The effect of contact time, initial Cd concentration, nano-hybrid dosage and temperature on the adsorption efficiency was fully evaluated. The adsorption data were well-fitted to the pseudo-second-order kinetic and Langmuir isotherm model with the maximum adsorption capacity of 35.36 mg/g. In the following, enthalpy, entropy and Gibbs free energy parameters of the Cd (II) ions adsorption were computed. Based on the activation parameters of the thermodynamic study, the adsorption of Cd(II) ions on the MBA nano-hybrid was spontaneous. The results of repeated adsorption–desorption cycles exhibited that MBA nano-hybrid can be effectively used as a recyclable adsorbent for the removal of Cd(II) from aqueous phase. Complementary experiments indicated that the as-prepared nano-hybrid can selectively adsorb Cd(II) ions in the presence of other competing cationic compounds. Conclusively, the MBA nano-hybrid can be proposed as an efficient adsorbent for treating Cd(II)-contaminated solutions. Actually, the results of the present study provide a promising treatment technique for the removal and also recovery of heavy metals from water and wastewater.

Data availability

The datasets used and/or analyzed in this study are available in the manuscript can be asked from the corresponding author upon request.

Received: 7 April 2022; Accepted: 30 June 2022

Published online: 06 July 2022

References

- Zeng, G. et al. Enhancement of Cd (II) adsorption by polyacrylic acid modified magnetic mesoporous carbon. *Chem. Eng. J.* **259**, 153–160 (2015).
- Gupta, V. & Nayak, A. Cadmium removal and recovery from aqueous solutions by novel adsorbents prepared from orange peel and Fe₂O₃ nanoparticles. *Chem. Eng. J.* **180**, 81–90 (2012).
- Soltani, R. D. C. et al. Preparation of chitosan/bone Char/Fe₃O₄nanocomposite for adsorption of hexavalent chromium in aquatic environments. *Arab. J. Sci. Eng.* **43**, 5799–5808 (2018).
- Ebrahimi, R. et al. Adsorptive removal of nickel and lead ions from aqueous solutions by poly (amidoamine) (PAMAM) dendrimers (G4). *Environ. Technol. Innov.* **12**, 261–272 (2018).
- Copello, G., Varela, F., Vivot, R. M. & Díaz, L. Immobilized chitosan as biosorbent for the removal of Cd (II), Cr (III) and Cr (VI) from aqueous solutions. *Bioresour. Technol.* **99**, 6538–6544 (2008).

6. Hossini, H., Rezaee, A., Rastegar, S. O., Hashemi, S. & Safari, M. Equilibrium and kinetic studies of chromium adsorption from wastewater by functionalized multi-wall carbon nanotubes. *React. Kinet. Mech. Catal.* **112**, 371–382 (2014).
7. Huang, Y. & Keller, A. A. EDTA functionalized magnetic nanoparticle sorbents for cadmium and lead contaminated water treatment. *Water Res.* **80**, 159–168 (2015).
8. Soltani, R. D. C., Jafari, A. J. & Khorramabadi, G. S. Investigation of cadmium (II) ions biosorption onto pretreated dried activated sludge. *Am. J. Environ. Sci.* **5**, 41–46 (2009).
9. Chen, A. *et al.* Novel thiourea-modified magnetic ion-imprinted chitosan/TiO₂ composite for simultaneous removal of cadmium and 2, 4-dichlorophenol. *Chem. Eng. J.* **191**, 85–94 (2012).
10. Gong, J. *et al.* Shellac-coated iron oxide nanoparticles for removal of cadmium (II) ions from aqueous solution. *J. Environ. Sci.* **24**, 1165–1173 (2012).
11. Gutiérrez-Segura, E., Solache-Ríos, M., Colín-Cruz, A. & Fall, C. Adsorption of cadmium by Na and Fe modified zeolitic tuffs and carbonaceous material from pyrolyzed sewage sludge. *J. Environ. Manage.* **97**, 6–13 (2012).
12. Yao, W., Rao, P., Lo, I. M., Zhang, W. & Zheng, W. Preparation of cross-linked magnetic chitosan with quaternary ammonium and its application for Cr (VI) and P (V) removal. *J. Environ. Sci.* **26**, 2379–2386 (2014).
13. Atar, N., Olgun, A. & Wang, S. Adsorption of cadmium (II) and zinc (II) on boron enrichment process waste in aqueous solutions: Batch and fixed-bed system studies. *Chem. Eng. J.* **192**, 1–7 (2012).
14. Li, X. *et al.* Novel magnetic beads based on sodium alginate gel crosslinked by zirconium(IV) and their effective removal for Pb²⁺ in aqueous solutions by using a batch and continuous systems. *Bioresour. Technol.* **142**, 611–619 (2013).
15. Mahmoud, M. E. & Al-Bishri, H. M. Supported hydrophobic ionic liquid on nano-silica for adsorption of lead. *Chem. Eng. J.* **166**, 157–167 (2011).
16. Soltani, R. D. C. *et al.* Application of nanocrystalline iranian diatomite in immobilized form for removal of a textile dye. *J. Dispers. Sci. Technol.* **37**, 723–732 (2016).
17. Zhu, Q. *et al.* Preparation and characterization of Cu₂O–ZnO immobilized on diatomite for photocatalytic treatment of red water produced from manufacturing of TNT. *Chem. Eng. J.* **171**, 61–68 (2011).
18. Dang, T. D. *et al.* Bio-silica coated with amorphous manganese oxide as an efficient catalyst for rapid degradation of organic pollutant. *Colloids Surf. B: Biointerfaces* **106**, 151–157 (2013).
19. Fernandez-Garcia, M., Martinez-Arias, A., Hanson, J. & Rodriguez, J. Nanostructured oxides in chemistry: characterization and properties. *Chem. Rev.* **104**, 4063–4104 (2004).
20. Mauter, M. S. & Elimelech, M. Environmental applications of carbon-based nanomaterials. *Environ. Sci. Technol.* **42**, 5843–5859 (2008).
21. Liu, Y., Chen, M. & Yongmei, H. Study on the adsorption of Cu (II) by EDTA functionalized Fe₃O₄ magnetic nano-particles. *Chem. Eng. J.* **218**, 46–54 (2013).
22. Soltani, R. D. C. *et al.* Decontamination of arsenic(V)-contained liquid phase utilizing Fe₃O₄/bone char nanocomposite encapsulated in chitosan biopolymer. *Environ. Sci. Pollut. Res.* **24**, 15157–15166 (2017).
23. Srivastava, M. *et al.* Synthesis of superparamagnetic bare Fe₃O₄ nanostructures and core/shell (Fe₃O₄/alginate) nanocomposites. *Carbohydr. Polym.* **89**, 821–829 (2012).
24. Zhao, Y. *et al.* Adsorption of Cu (II) and Cd (II) from wastewater by sodium alginate modified materials. *J. Chem.* **2020**, 1–13 (2020).
25. Lou, Z. *et al.* Magnetized bentonite by Fe₃O₄ nanoparticles treated as adsorbent for methylene blue removal from aqueous solution: Synthesis, characterization, mechanism, kinetics and regeneration. *J. Taiwan Inst. Chem. Eng.* **49**, 199–205 (2016).
26. Soltani, R. D. C., Khataee, A. R., Safari, M. & Joo, S. W. Preparation of bio-silica/chitosan nanocomposite for adsorption of a textile dye in aqueous solutions. *Int. Biodeterior. Biodegrad.* **85**, 383–391 (2013).
27. Soltani, R. D. C. *et al.* Response surface methodological evaluation of the adsorption of textile dye onto biosilica/alginate nanobiocomposite: thermodynamic, kinetic, and isotherm studies. *Desalin. Water Treat.* **56**, 1389–1402 (2015).
28. Soltani, R. D. C., Jorfi, S., Ramezani, H. & Purfadakari, S. Ultrasonically induced ZnO–biosilica nanocomposite for degradation of a textile dye in aqueous phase. *Ultrason. Sonochem.* **28**, 69–78 (2016).
29. Hassani, A., Soltani, R. D. C., Karaca, S. & Khataee, A. Preparation of montmorillonite–alginate nanobiocomposite for adsorption of a textile dye in aqueous phase: Isotherm, kinetic and experimental design approaches. *J. Ind. Eng. Chem.* **21**, 1197–1207 (2015).
30. Hosseini, S. S., Pasalari, H., Yousefi, N. & Mahvi, A. H. Eggshell modified with alum as low-cost sorbent for the removal of fluoride from aquatic environments: isotherm and kinetic studies. *Desalin. Water Treat.* **146**, 326–332 (2019).
31. Bayramoglu, G. & Arica, M. Y. Preparation of a composite biosorbent using scenedesmus quadricauda biomass and alginate/polyvinyl alcohol for removal of Cu(II) and Cd(II) ions: isotherms, kinetics, and thermodynamic studies. *Water, Air, and Soil Pollut.* **221**, 391–403 (2011).
32. Shen, Y. *et al.* Microalgal-biochar immobilized complex: a novel efficient biosorbent for cadmium removal from aqueous solution. *Bioresour. Technol.* **244**, 1031–1038 (2017).
33. Alakhras, F. Biosorption of Cd (II) ions from aqueous solution using chitosan-iso-vanillin as a low-cost sorbent: equilibrium, kinetics, and thermodynamic studies. *Arab. J. Sci. Eng.* **44**, 279–288 (2019).
34. Dolgormaa, A. *et al.* Adsorption of Cu(II) and Zn(II) Ions from aqueous solution by Gel/PVA-modified super-paramagnetic iron oxide nanoparticles. *Molecules* **23**, 2982 (2018).
35. Yagub, M. T., Sen, T. K., Afroze, S. & Ang, H. M. Dye and its removal from aqueous solution by adsorption: a review. *Adv. Colloid Interface Sci.* **209**, 172–184 (2014).
36. Benhima, H., Chiban, M., Sinan, F., Seta, P. & Persin, M. Removal of lead and cadmium ions from aqueous solution by adsorption onto micro-particles of dry plants. *Colloids Surf. B Biointerfaces* **61**, 10–16 (2008).
37. Wang, H., Wang, X., Ma, J., Xia, P. & Zhao, J. Removal of cadmium (II) from aqueous solution: A comparative study of raw attapulgite clay and a reusable waste–struvite/attapulgite obtained from nutrient-rich wastewater. *J. Hazard. Mater.* **329**, 66–76 (2017).
38. Pasalari, H., Ghaffari, H. R., Mahvi, A. H., Pourshabanian, M. & Azari, A. Activated carbon derived from date stone as natural adsorbent for phenol removal from aqueous solution. *Desalin. Water Treat.* **72**, 406–417 (2017).
39. Safari, M., Khataee, A., Soltani, R. D. C. & Rezaee, R. Ultrasonically facilitated adsorption of an azo dye onto nanostructures obtained from cellulosic wastes of broom and cooler straw. *J. Colloid Interface Sci.* **522**, 228–241 (2018).
40. Yousefi, M. *et al.* Modification of pumice with HCl and NaOH enhancing its fluoride adsorption capacity: kinetic and isotherm studies. *Hum Ecol Risk Assess.* **25**, 1508–1520 (2019).
41. Badruddoza, A. Z. M., Shawon, Z. B. Z., Tay, W. J. D., Hidajat, K. & Uddin, M. S. Fe₃O₄/cyclodextrin polymer nanocomposites for selective heavy metals removal from industrial wastewater. *Carbohydr. Polym.* **91**, 322–332 (2013).
42. Yi, X. *et al.* Encapsulating Fe₃O₄ into calcium alginate coated chitosan hydrochloride hydrogel beads for removal of Cu (II) and U (VI) from aqueous solutions. *Ecotoxicol. Environ. Saf.* **147**, 699–707 (2018).
43. Yi, X. *et al.* Graphene oxide encapsulated polyvinyl alcohol/sodium alginate hydrogel microspheres for Cu (II) and U (VI) removal. *Ecotoxicol. Environ. Saf.* **158**, 309–318 (2018).
44. Wei, C., Song, X., Wang, Q. & Hu, Z. Sorption kinetics, isotherms and mechanisms of PFOS on soils with different physicochemical properties. *Ecotoxicol. Environ. Saf.* **142**, 40–50 (2017).
45. Hassani, A., Kiransan, M., Soltani, R. D. C., Khataee, A. & Karaca, S. Optimization of the adsorption of a textile dye onto nanoclay using a central composite design. *Turk J. Chem.* **39**, 734–749 (2015).

46. Liu, Y. *et al.* Multifunctional nanocomposites Fe₃O₄@SiO₂-EDTA for Pb (II) and Cu (II) removal from aqueous solutions. *Appl. Surf. Sci.* **369**, 267–276 (2016).
47. Sheikhmohammadi, A. *et al.* The synthesis and application of the Fe₃O₄@SiO₂ nanoparticles functionalized with 3-aminopropyltriethoxysilane as an efficient sorbent for the adsorption of ethylparaben from wastewater: Synthesis, kinetic, thermodynamic and equilibrium studies. *J. Environ. Chem. Eng.* **7**, 103315 (2019).
48. Soltani, R. D. C., Rezaee, A., Khorramabadi, G. S. & Yaghmaian, K. Technology: optimization of lead (II) biosorption in an aqueous solution using chemically modified aerobic digested sludge. *Water Sci. Technol.* **63**, 129–135 (2011).
49. Li, C., Duan, H., Wang, X., Meng, X. & Qin, D. Fabrication of porous resins via solubility differences for adsorption of cadmium (II). *Chem. Eng. J.* **262**, 250–259 (2015).
50. Duan, J. & Su, B. Removal characteristics of Cd (II) from acidic aqueous solution by modified steel-making slag. *Chem. Eng. J.* **246**, 160–167 (2014).
51. Liu, C., Wu, P., Zhu, Y. & Tran, L. Simultaneous adsorption of Cd²⁺ and BPA on amphoteric surfactant activated montmorillonite. *Chemosphere* **144**, 1026–1032 (2016).
52. Dang, V. B. H., Doan, H. D., Dang-Vu, T. & Lohi, A. Equilibrium and kinetics of biosorption of cadmium(II) and copper(II) ions by wheat straw. *Bioresour. Technol.* **100**, 211–219 (2009).
53. Wang, F. Y., Wang, H. & Ma, J. W. Adsorption of cadmium (II) ions from aqueous solution by a new low-cost adsorbent—Bamboo charcoal. *J. Hazard. Mater.* **177**, 300–306 (2010).
54. Phuengprasop, T., Sittiwong, J. & Unob, F. Removal of heavy metal ions by iron oxide coated sewage sludge. *J. Hazard. Mater.* **186**, 502–507 (2011).
55. Ulmanu, M. *et al.* Removal of copper and cadmium ions from diluted aqueous solutions by low cost and waste material adsorbents. *Water, air, and soil poll.* **142**, 357–373 (2003).
56. Fan, F.-L. *et al.* Rapid removal of uranium from aqueous solutions using magnetic Fe₃O₄@SiO₂ composite particles. *J. Environ. Radioact.* **106**, 40–46 (2012).
57. Cheng, C., Wang, J., Yang, X., Li, A. & Philippe, C. Adsorption of Ni (II) and Cd (II) from water by novel chelating sponge and the effect of alkali-earth metal ions on the adsorption. *J. Hazard. Mater.* **264**, 332–341 (2014).
58. Fakhri, H., Mahjoub, A. R. & Aghayan, H. Preparation of nanocomposite heteropoly metalate based graphene oxide: Insight into cadmium adsorption. *J. Nanostruct.* **7**, 223–235 (2017).
59. Sheikhmohammadi, A. *et al.* Fabrication of magnetic graphene oxide nanocomposites functionalized with a novel chelating ligand for the removal of Cr (VI): Modeling, optimization, and adsorption studies. *Desalin. Water Treat.* **160**, 297–307 (2019).
60. Sheikhmohammadi, A. *et al.* Application of graphene oxide modified with the phenopyridine and 2-mercaptobenzothiazole for the adsorption of Cr (VI) from wastewater: Optimization, kinetic, thermodynamic and equilibrium studies. *J. Mol. Liq.* **285**, 586–597 (2019).
61. Witek-Krowiak, A. Application of beech sawdust for removal of heavy metals from water: biosorption and desorption studies. *Eur. J. Wood Wood Prod.* **71**, 227–236 (2013).
62. Rasoulzadeh, H., Mohseni-Bandpei, A., Hosseini, M. & Safari, M. Mechanistic investigation of ciprofloxacin recovery by magnetite-imprinted chitosan nanocomposite: Isotherm, kinetic, thermodynamic and reusability studies. *Int. J. Biol. Macromol.* **133**, 712–721 (2019).
63. Cechinel, M. A. P., de Souza, S. M. A. G. U. & de Souza, A. A. U. Study of lead (II) adsorption onto activated carbon originating from cow bone. *J. Clean. Prod.* **65**, 342–349 (2014).

Acknowledgements

The authors thank Kurdistan University of Medical Sciences, Sanandaj (Iran) for providing financial and instrumental supports (Grant number: 94/287).

Author contributions

The manuscript was written through contributions of all authors. All authors have given approval to the final version of the manuscript. Mahdi Safari: Investigation, Conceptualization, Writing - original draft. Reza Rezaee: Supervision, Methodology. Reza Darvishi Cheshmeh Soltani: Methodology, writing - review & editing, Resources. Esrafil Asgari: Resources, Visualization, Formal analysis.

Competing interests

The authors declare no competing interests.

Additional information

Correspondence and requests for materials should be addressed to E.A.

Reprints and permissions information is available at www.nature.com/reprints.

Publisher's note Springer Nature remains neutral with regard to jurisdictional claims in published maps and institutional affiliations.



Open Access This article is licensed under a Creative Commons Attribution 4.0 International License, which permits use, sharing, adaptation, distribution and reproduction in any medium or format, as long as you give appropriate credit to the original author(s) and the source, provide a link to the Creative Commons licence, and indicate if changes were made. The images or other third party material in this article are included in the article's Creative Commons licence, unless indicated otherwise in a credit line to the material. If material is not included in the article's Creative Commons licence and your intended use is not permitted by statutory regulation or exceeds the permitted use, you will need to obtain permission directly from the copyright holder. To view a copy of this licence, visit <http://creativecommons.org/licenses/by/4.0/>.

© The Author(s) 2022